INTERNATIONAL JOURNAL FOR NUMERICAL METHODS IN FLUIDS, VOL. 3, 567–581 (1983)

FRACTIONAL STEP ALGORITHM FOR ESTUARINE MASS TRANSPORT

R. J. SOBEY

Department of Civil and Systems Engineering, James Cook University, Townsville Q. 4811, Australia.

SUMMARY

A successful and economical fractional step algorithm for the convection–dispersion–reaction equation is described. Exact solutions are adopted for the reaction and convection steps, the latter by the introduction of a moving co-ordinate system. The dispersion step uses an optimized finite difference algorithm which specifically accommodates the grid non-uniformity. The excellent performance of the algorithm is confirmed by numerical experiments together with computations of the Fourier response and integrated square error characteristics.

KEY WORDS Advection Convection Estuary Fractional Step Diffusion Dispersion Moving Co-ordinates Transport

INTRODUCTION

Estuarine mass transport is essentially a convective transport problem and any numerical solution algorithm that maintains an Eulerian framework has potential problems with numerical dispersion and solution oscillations. It is generally recognized that the numerical difficulties originate with the convective term and are particularly severe where there is poor spatial resolution, although there is little agreement regarding the most satisfactory solution algorithm. Numerous algorithms have been proposed in the literature and all three appropriate numerical solution techniques—the method of characteristics, the finite difference method and the finite element method—have been used in a wide variety of forms. This paper describes a fractional step algorithm that achieves reasonable precision without recourse to higher order approximations. Each fractional step describes one of the three physical processes contributing to estuarine mass transport, respectively convection, dispersion and chemical reaction. Essentially exact solutions are adopted for the convection and reaction steps and an optimized difference scheme is used for the dispersion step. Fourier mode analyses and numerical experiments confirm the excellent performance of the algorithm.

The context of this study was mass transport in a narrow but well-mixed estuarine channel. In typical applications the single reach considered might be one link in a link-node model of estuarine mass transport. Estuarine conditions provide a severe test of any solution algorithm. Flows may vary from nothing to large values in both directions and concentration gradients may vary in a similar manner. A successful algorithm must accommodate this range of operational conditions. In dimensionless terms with the local space step Δx and the time step Δt as the characteristic length and time scales, the numerical solution is dependent on the flow parameter $U\,\Delta t/\Delta x$ and the dispersion parameter $E\,\Delta t/\Delta x^2$, where $U(x, t)$ is the cross-sectionally averaged flow velocity including tidal and fresh-water components and E is

0271–2091/83/060567–15$01.50

Received 23 October 1981
Revised 21 August 1982

the longitudinal dispersion coefficient. In a typical estuarine situation the flow parameter might range in magnitude up to about three and the dispersion parameter would be small and of order 0·01.

FRACTIONAL STEPS

In the numerical solution of initial problems involving a number of transport directions and/or interacting influences, the fractional step method[1,2] can often be used to advantage. It is applicable to initial value problems in a dependent variable u, that can be written as

$$\frac{\partial u}{\partial t} = L[u] \tag{1}$$

where L is an operator and the sum of p separate operations

$$L = L_1 + L_2 + \ldots + L_p \tag{2}$$

The numerical solution of equation (1) over a time step Δt is achieved by p fractional steps, each of duration $\Delta t/p$ and being numerical solutions of the consecutive initial value problems

$$\frac{\partial u}{\partial t} = pL_i[u] \quad \text{for} \quad i = 1, 2 \ldots p \tag{3}$$

In this way a potentially complicated problem is replaced by a succession of simpler problems. The complication may be a number of transport directions and/or a number of interacting influences. The simpler fractional problem usually involves a single spatial direction and a single influence on the time history of the dependent variable. The major advantage of the fractional step method is the separate consideration given to each fractional step, allowing the adoption of a numerical algorithm appropriate for that step and not forcing the adoption of a single algorithm for the complete problem. The well known alternating direction implicit (A.D.I.) algorithm for the numerical solution of propagation problems in two spatial dimensions is an example of the fractional step method.

Estuarine mass transport for a variable cross-section but well-mixed, one dimensional channel is described by the equation

$$\frac{\partial}{\partial t}(AC) + \frac{\partial}{\partial x}(QC) = \frac{\partial}{\partial x}\left(AE\frac{\partial C}{\partial x}\right) - KAC - AS \tag{4}$$

where $C(x, t)$ is the slowly-varying concentration of the dispersive substance, t is time, x is the longitudinal co-ordinate along the estuarine channel, $Q(x, t)$ is the known channel discharge, $A(x, t)$ is the cross-sectional area of the channel, K is the linear reaction rate coefficient for the particular substance and S is a source or sink for that substance. Separating out component terms, using the continuity equation

$$\frac{\partial A}{\partial t} + \frac{\partial Q}{\partial x} = 0 \tag{5}$$

for the channel flow, neglecting the small non-linear term $\dfrac{\partial A}{\partial x}\dfrac{\partial C}{\partial x}$ and assuming E is constant reduces equation (4) to

$$\frac{\partial C}{\partial t} + \frac{Q}{A}\frac{\partial C}{\partial x} = E\frac{\partial^2 C}{\partial x^2} - KC - S \tag{6}$$

which is the classical one-dimensional convection–dispersion-reaction equation.

In the context of a fractional step method, equation (6) becomes

$$\frac{\partial C}{\partial t} = (L_1 + L_2 + L_3)[C] \tag{7}$$

where

$$L_1[C] = -KC - S \tag{8}$$

$$L_2[C] = -\frac{Q}{A}\frac{\partial C}{\partial x} \tag{9}$$

and

$$L_3[C] = E\frac{\partial^2 C}{\partial x^2} \tag{10}$$

The separate fractional steps describe the three physical processes contributing to the estuarine mass balance, respectively reaction, convection and dispersion. The specific advantage of the fractional step method in allowing separate numerical solution algorithms for each step immediately identifies the convection step as the potential source of problems. Successful numerical algorithms for the reaction and dispersion steps are available but numerical algorithms for convective transport problems frequently encounter serious numerical dispersion and solution oscillations. The fractional step method allows specific consideration to be given to this problem without the need to simultaneously accommodate the reaction and dispersion steps.

REACTION STEP

The reaction step is the initial value problem

$$\frac{\partial C}{\partial t} = -3(KC + S) \tag{11}$$

from $n\,\Delta t$ to $(n+\frac{1}{3})\,\Delta t$. A numerical solution of this step is unnecessary as an analytical solution is available:[3]

$$C^{n+\frac{1}{3}} = C^n \exp(-K\,\Delta t) - S\,\Delta t\left[\frac{1-\exp(-K\,\Delta t)}{K\,\Delta t}\right] \tag{12}$$

Problems with the square bracketed term for K equal to zero or very small may be accommodated by use of the series expansion

$$\frac{1-\exp(-K\,\Delta t)}{K\,\Delta t} = 1 - \frac{K\,\Delta t}{2!} + \frac{(K\,\Delta t)^2}{3!} - \frac{(K\,\Delta t)^3}{4!} \cdots \tag{13}$$

Both K and S typically vary slowly with time, if at all, and little difficulty is introduced by assuming constant values over each time step.

CONVECTION STEP

The convection step is the initial value problem

$$\frac{\partial C}{\partial t} + 3\frac{Q}{A}\frac{\partial C}{\partial x} = 0 \tag{14}$$

from $(n+\frac{1}{3})\Delta t$ to $(n+\frac{2}{3})\Delta t$. Using the method of characteristics, this partial differential equation is equivalent to the pair of ordinary differential equations

$$\frac{dC}{dt}=0 \tag{15}$$

and

$$\frac{dx}{dt}=3\frac{Q}{A} \tag{16}$$

Hence concentration is constant along characteristic lines in the solution field described by equation (16). The exact nature of this solution can only be realized by following the characteristics. Reference back to a fixed Eulerian grid transforms the problem to one of interpolation for C between nodes at time $(n+\frac{1}{3})\Delta t$, which in turn introduces numerical dispersion and solution oscillations as demonstrated by Fromm[4] and Holly and Preissman.[5]

An exact solution must follow the characteristics, requiring the adoption of a moving co-ordinate system defined by integration of equation (16). In general both Q and A vary with position and time in a manner normally predicted by a coupled numerical hydrodynamic model on a uniform $\Delta x, \Delta t$ grid. The characteristic paths may be followed by numerical integration of equation (16) using the Runge–Kutta method with Q and A determined by linear spatial and temporal interpolation from the normally uniform grid of the numerical hydrodynamic model. Only where Q and A are both constant throughout the solution field are the characteristic lines parallel and can a uniform grid be retained. This is not the usual situation for a real estuary and a spatially non-uniform grid is a direct consequence, as sketched in Figure 1. With this moving co-ordinate system, the numerical solution for the convection step becomes

$$C_i^{n+\frac{2}{3}}=C_i^{n+\frac{1}{3}} \tag{17}$$

the subscript i identifying x_i, the spatial position of the ith node in the moving co-ordinate system.

There is little difficulty in accommodating the boundary conditions in the context of the moving co-ordinate system even though they are specified at fixed positions. In parabolic problems such as this a clear distinction must be made between inflow and outflow boundaries. For inflow boundaries the boundary conditions must be specified to the solution field and a new node is initiated at the boundary each time step. In contrast, outflow

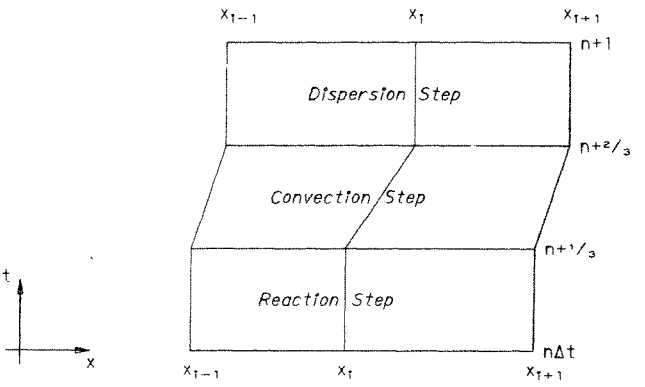

Figure 1. Fractional step grid

boundaries are computed from the solution field by means of the outflow characteristic to the boundary node at the new time. This is essentially the same procedure that is followed for an Eulerian grid.

DISPERSION STEP

The dispersion step is the initial value problem

$$\frac{\partial C}{\partial t} = 3E\frac{\partial^2 C}{\partial x^2} \tag{18}$$

from $(n+\frac{2}{3})\,\Delta t$ to $(n+1)\,\Delta t$. Dispersion is frequently the least important of estuarine transport processes and reasonably accurate numerical solutions over a uniform grid are quite straightforward. In the estuarine environment however the convective transport (i.e. U or Q/A) is not constant but varies with position and time. As a consequence, the moving co-ordinate system adopted for the convection step will give rise to a generally non-uniform but still rectangular grid over which the dispersion step must be accommodated, as shown in Figure 1.

It is apparent, just from arguments of symmetry, that the asymmetry of the grid must be considered in the development of a suitable numerical algorithm. An appropriate algorithm is described in a companion paper.[6] The asymmetric grid on which the algorithm is based is sketched in Figure 2. Centered Taylor series expansions are written for each of the six nodes of the local double cell and the following lowest-order finite difference equation was established by elimination among the nodes:

$$\left[\frac{1}{2}-\frac{\phi}{1+A}\right]C_{i+1}^{n+1}+\left[\frac{2\phi}{1-A^2}\right]C_i^{n+1}+\left[\frac{1}{2}-\frac{\phi}{1-A}\right]C_{i+1}^{n+1}$$
$$=\left[\frac{1}{2}-\frac{\phi}{1+A}+\frac{E'}{1+A}\right]C_{i-1}^{n}+\left[\frac{2\phi}{1-A^2}-\frac{2E'}{1-A}\right]C_i^{n}+\left[\frac{1}{2}-\frac{\phi}{1-A}+\frac{E'}{1-A}\right]C_{i+1}^{n} \tag{19}$$

where A is the local grid asymmetry defined as $(x_i - x_{i-1} - \Delta x)/2$, Δx being defined as $(x_{i+1} - x_{i-1})/2$, E' is written for $E\,\Delta t/\Delta x^2$ and

$$\phi = (1-A^2)\beta/2 + (E\,\Delta t/\Delta x^2)\delta \tag{20}$$

where β and δ are independent weighting parameters associated with the time and space derivatives in equation (18). The weighting parameters β and δ appear in the discrete equation only in the combination indicated by equation (20), so that they are not independent and may be represented by a single parameter ϕ, which is also dependent on the

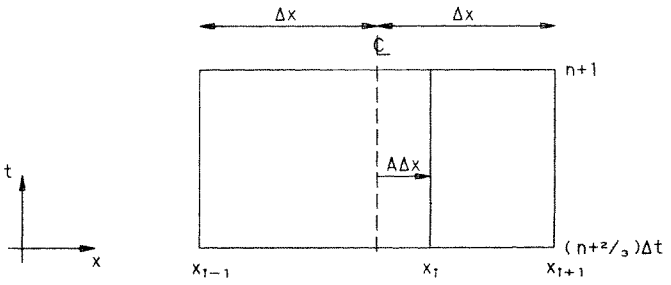

Figure 2. Asymmetric grid for dispersion step

asymmetry and dispersion parameters. Noting that ϕ is essentially a free parameter whose magnitude does not affect either consistency or convergence of equation (19), it has been shown by Sobey[6] that ϕ can be chosen such that the accuracy of the algorithm is optimized, in the sense that the integrated square error is a minimum. The parameter ϕ for the optimized algorithm is a function of the dispersion parameter and the magnitude of the asymmetry; the $\phi(A, E\,\Delta t/\Delta x^2)$ surface is presented in Reference 6. This procedure accommodates grid asymmetry and maintains reasonable accuracy without recourse to higher order approximations. Numerical experiments and computations of the Fourier response factor described also in Reference 6 confirmed the performance of this optimized asymmetric algorithm.

ADDITION AND REMOVAL OF NODES

In response to a space and time variable flow field, the moving co-ordinate system adopted for the convection step can result in convergence and divergence of nodes to such an extent that it becomes computationally desirable to add or remove certain nodes. In simultaneously accommodating the boundary conditions, it is first necessary to keep track of those nodes remaining within the solution field. Nodes are initiated at inflow boundaries and propagate from the solution field at outflow boundaries. Convergence of nodes within the solution field may result in more resolution in a particular region then is really necessary to adequately describe the local response. Alternatively, divergence of nodes may result in insufficient resolution of the local response. In both cases the local asymmetry may become too extreme to be reasonably accommodated by the dispersion step.

Removal of nodes poses no computational problems but the addition of nodes must use linear interpolation. Some rational basis for the addition and removal of nodes is necessary, for which appropriate criteria would be the simultaneous maintenance of adequate resolution and moderate asymmetry.

If dx is defined as the target space step judged necessary to achieve adequate overall resolution of the physical problem, then generalized acceptance criteria for local node spacings can be expressed as

$$r\,dx < \Delta x < a\,dx \tag{21}$$

$$(1 - A_{max})\,\Delta x < x_i - x_{i-1} < (1 + A_{max})\,\Delta x \tag{22}$$

where Δx is $(x_{i+1} - x_{i-1})/2$ as above, and suitable values for r, a and A_{max} are 0·5, 2·0 and +0·75, respectively. Nodes are added or removed from the solution field as necessary to satisfy both conditions.

In a general sense it should be noted that convergence and divergence of nodes within the solution field would normally enhance the performance of the algorithm. Sharp gradients of concentration are frequently a consequence of nodal convergence and the additional spatial resolution is certainly an advantage here. The reverse is normally the case with nodal divergence. This natural accommodation of spatial resolution is not essential to the performance of the fractional step algorithm but it is certainly an additional advantage of the approach.

FOURIER MODE ANALYSIS

It is well recognized that any numerical algorithm is most successful in accommodating the longer spatial wave lengths and often quite inadequate for shorter wave lengths. This is a

problem with all discrete approximations, regardless of the numerical method adopted, but it is not normally troublesome if there is adequate spatial resolution. However, sharp concentration gradients are frequently encountered in estuarine mass transport and there is consequently considerable interest in the short wave length performance. No numerical algorithm can resolve spatial Fourier components with wavelengths less than $L_N = 2\Delta x$ or wave numbers $\sigma = 2\pi/L$ greater than $\sigma_N = \pi/\Delta x$, termed the Nyquist limit. The performance of wave numbers up to the Nyquist limit is best described by a Fourier mode or wave deformation analysis, which compares Fourier series solutions to both the partial differential equation and the numerical algorithm.

The physical solution is the solution to the partial differential equation (6), represented as the real part of the Fourier series

$$C(x, t) = \sum_m C_m^* \exp[\mathrm{i}(\beta_m t + \sigma_m x)] \tag{23}$$

where β_m ($=2\pi/T_m$, T_m being the wave period) is the wave angular frequency and σ_m ($=2\pi/L_m$, L_m being the wavelength) the spatial wave number of the mth Fourier component. Equation (6) is linear, so that only one component of equation (23) need be considered at a time. Substitution of a single Fourier component, $C^* \exp[\mathrm{i}(\beta t + \sigma x)]$, into equation (6) establishes the dispersion relationship for the physical wave

$$\beta = -\sigma U + \mathrm{i}[\sigma^2 E + K]$$

or

$$\beta\,\Delta t = (\sigma\,\Delta x)\frac{U\,\Delta t}{\Delta x} + \mathrm{i}\left[(\sigma\,\Delta x)^2 \frac{E\,\Delta t}{\Delta x^2} + K\,\Delta t\right] \tag{24}$$

where U is written for Q/A.

The numerical solution is the solution to the complete fractional step algorithm which is also represented as the real part of a Fourier series

$$C_i^n = \sum_m C_m^* \exp[\mathrm{i}(\beta_m' t + \sigma_m x)] \tag{25}$$

along the lines of equation (23) but allowing the angular wave frequencies β_m' to be complex and different from β_m for the physical solution. Equations (12), (17) and (19) are also linear so that only one component of equation (25) need be considered at a time. Equations (12) and (17) are exact and numerical error is introduced only through the dispersion step. Substitution of a single Fourier component, $C^* \exp[\mathrm{i}(\beta' t + \sigma x)]$, into equation (19) gives

$$\exp(\mathrm{i}\beta'\,\Delta t) = 1 + \frac{zE\,\Delta t/\Delta x^2}{\cos(\sigma\,\Delta x) - \phi z} \tag{26}$$

where

$$z = \frac{\exp(-\mathrm{i}\sigma\,\Delta x)}{1+A} - \frac{2\exp(\mathrm{i}\,A\sigma\,\Delta x)}{1-A^2} + \frac{\exp(\mathrm{i}\sigma\,\Delta x)}{1-A}$$

This is the equivalent dispersion relationship for the numerical or computed wave for the complete fractional step algorithm.

The ratio of the computed solution to the physical solution after a specified time is called the propagation factor T, after Leendertse:[7]

$$T = \frac{\exp[\mathrm{i}(\beta' t + \sigma x)]}{\exp[\mathrm{i}(\beta t + \sigma x)]} = \exp[\mathrm{i}(\beta' - \beta)t] \tag{27}$$

Leendertse's terminology referred to long wave propagation and T can more appropriately be termed a Fourier response factor in the present context. Leendertse's choice of time scale was $2\pi/\beta$ for long wave propagation but β is complex in the present context and time must be real and positive. An appropriate choice for time in equation (27) is $2\pi/\mathrm{Re}(\beta) = 2\pi/(-\sigma U)$ as the present problem is convection-dominated. Note that this time is indeed positive because the positive direction for U opposes the positive direction implicit in the Fourier series expansions. Where T equals one, the solutions of the fractional step algorithm and partial differential equations are identical. The proximity of T to unity over the complete wave number spectrum is an established and convenient measure of the precision of a numerical algorithm.

The Fourier response factor thus defined depends on four dimensionless parameters: the flow parameter $U\,\Delta t/\Delta x$, the dispersion parameter $E\,\Delta t/\Delta x^2$,the asymmetry A and the dimensionless wave number $\sigma\Delta x = 2\pi/(L\,\Delta x)$. For a specific local numerical solution, the flow parameter, the dispersion parameter and the asymmetry are constant and the complete spectrum of behaviour is established by varying the dimensionless wave number $\sigma\,\Delta x$, or more commonly the dimensionless wave length $L/\Delta x$, over the full range. The dimensionless wave number or wavelength is a measure of the steepness of the concentration gradient. A small value of $L/\Delta x$ implies a steep gradient and this is where problems are anticipated.

A typical result is shown in Figure 3 for a moderate flow parameter of 0·5 and a typical dispersion parameter of 0·01. The reaction parameter $K\,\Delta t$ and the source/sink parameter $S\,\Delta t$ are usually small and have little influence on the performance of any numerical algorithm for the convection–dispersion–reaction equation. They were both set to zero. The parameter of these curves is the asymmetry and the solid lines show the variation in the Fourier response factor for asymmetries in the range 0·0 to ±0·9. The phase performance is excellent throughout but there is some small amplitude decay at very short wavelengths as the asymmetry becomes quite extreme. The dashed curve is included to give some perspective to the performance of the fractional step algorithm. It is the Fourier response for a linear space-time finite algorithm[8] for the same flow and dispersion parameters but for a uniform grid ($A = 0{\cdot}0$). The discrete equations for this algorithm are identical with the finite difference scheme of Stone and Brian[9] so that this result represents potentially the best available numerical algorithm on an Eulerian grid that maintains the lowest possible order of approximation. Higher order approximations on an Eulerian grid may yield better results than the dashed curve but at an added computational cost. The lowest order Eulerian grid algorithm is a reasonable comparison with the fractional step algorithm, which is also a lowest order approximation. The computational costs are certainly similar. Although the amplitude response of the Eulerian grid algorithm is comparable, the phase response deteriorates quite markedly at short wavelengths. The poor phase response has been identified[8] as the source of numerical dispersion and solution oscillation problems with such algorithms, as is further discussed below.

A single diagram like Figure 3 gives no indication of an algorithm's performance over the full operational range. The integrated square error[6]

$$S = \int_0^{\pi} [\mathrm{Re}(T) - 1]^2 \,\mathrm{d}(\sigma\,\Delta x) \tag{28}$$

is a single number measure of the performance of a numerical algorithm. The difference $\mathrm{Re}(T) - 1$ should be small under ideal circumstances and S is an objective and dimensionless measure of the overall error over all possible wave numbers. The performance of any

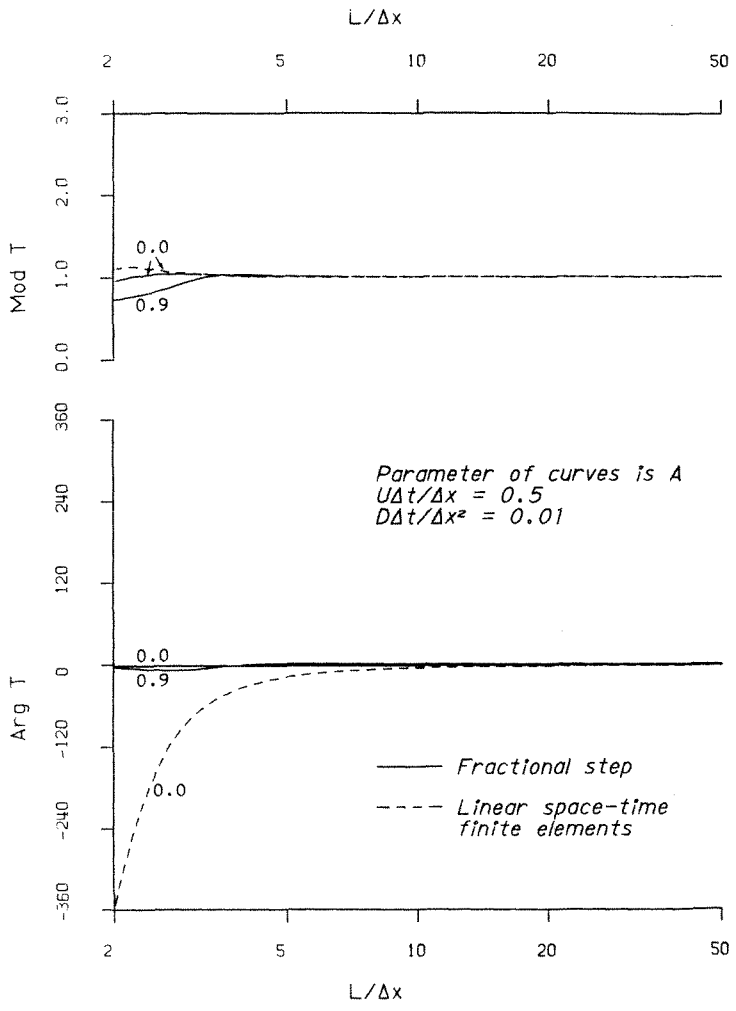

Figure 3. Fourier response factors for fractional step algorithm and Eulerian grid

numerical algorithm for the convection–dispersion–reaction equation is most dependent on the flow and dispersion parameters and Figure 4 shows the integrated square error for the fractional step algorithm as a function of $U\,\Delta t/\Delta x$ and $E\,\Delta t/\Delta x^2$ over a large part of the active parameter range. Once again the reaction and source/sink parameters have been set to zero. These two parameters have little influence on numerical performance and will not be further considered here. They are very significant, however, in the real environment.

Where the solution space remains convection-dominated ($E\,\Delta t/\Delta x^2 \lesssim 0{\cdot}1$), the integrated square error is very small and the performance of the fractional step algorithm must be rated as excellent. As the dispersion parameter increases beyond 1·0, the solution space becomes dispersion-dominated and the integrated square error increases rapidly, especially at low flow parameters where the dispersion dominance is more pronounced. A higher order approximation for the dispersion step might be necessary in this region of solution space but the present algorithm was not developed for a dispersion-dominated flow which would be very rare in an estuarine context. The equivalent result for the Eulerian grid algorithm introduced above is

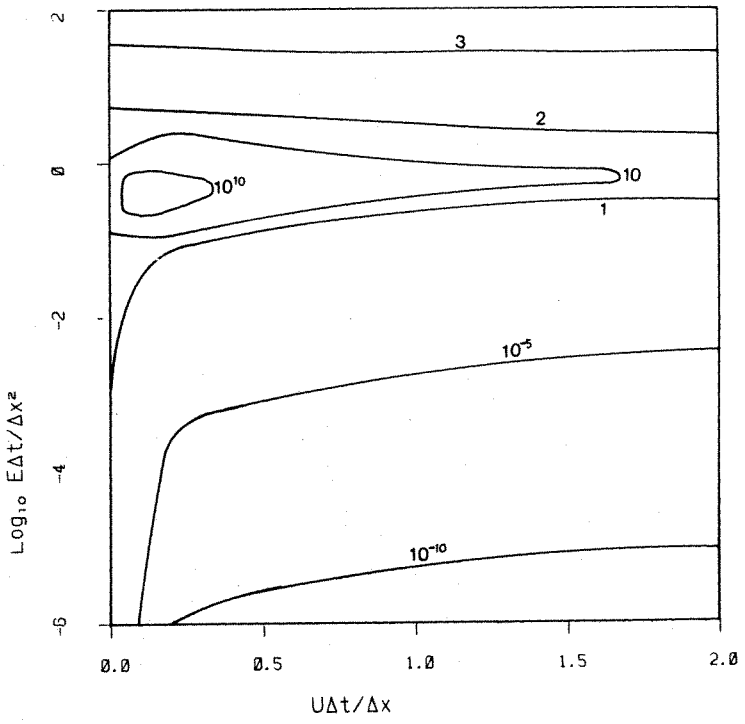

Figure 4. Integrated square error for fractional step algorithm

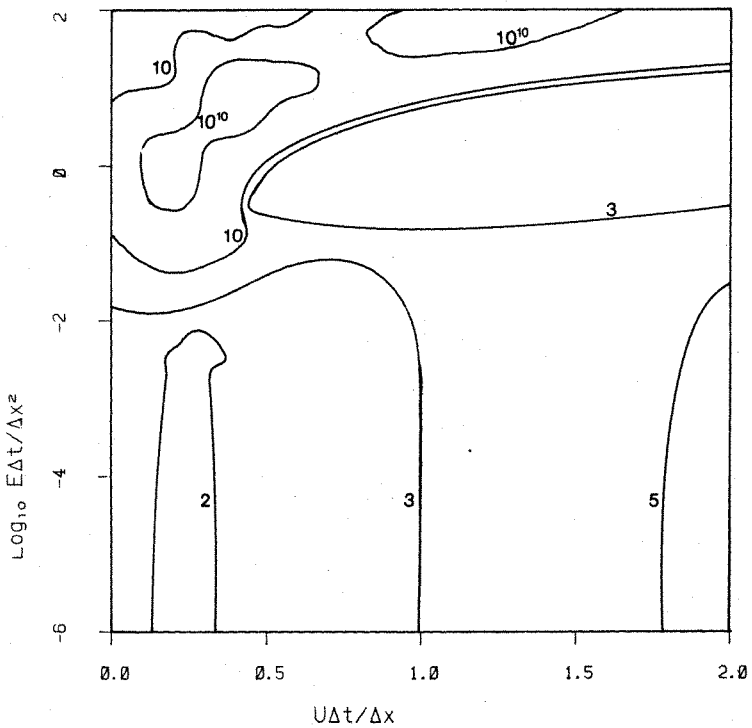

Figure 5. Integrated square error Eulerain grid

shown in Figure 5 and quite clearly demonstrates the markedly better performance of the fractional step algorithm where the solution space is dominated by the convection. The fractional step algorithm also performs better in much of the dispersion-dominated region of solution space. The response trends at very low and very large flow parameters are also noteworthy. There is a singularity in the Fourier response factor at $U\,\Delta t/\Delta x = 0{\cdot}0$ that is a consequence of the dependence of the time scale on the inverse of the flow parameter. This is responsible for some crowding of the isolines of S against the left-hand axis. The integrated square error response as $U\,\Delta t/\Delta x$ increases is particularly interesting in the convention-dominated region. For the fractional step algorithm the integrated square error increases very slowly but remains everywhere very small. For the Eulerian grid algorithm the integrated square error increases moderately rapidly towards the right, indicating significant deterioration in performance as the flow parameter increases.

NUMERICAL EXPERIMENTS

The final evaluation of the fractional step algorithm was a set of numerical experiments comparing the performance with an analytical solution to equation (6). Reaction and source/sink terms were neglected in these tests and the context is the convection and dispersion of an instantaneous point source of mass M at time zero. The analytical solution is

$$C(x, t) = \frac{M}{\rho A\sqrt{(4\pi E t)}} \exp\left[-\frac{(x-\bar{x})^2}{4Et}\right] \tag{29}$$

where $\bar{x}$ is the centroid of the pollutant cloud estimated from integration of

$$\frac{\mathrm{d}\bar{x}}{\mathrm{d}t} = U(x, t) \tag{30}$$

subject to initial conditions $\bar{x} = 0$ for $x = 0$, $t = 0$. For $U(x, t)$ constant, $\bar{x} = Ut$. In equation (29), ρ is the mass density of the water and A the constant cross-section of the channel. Equation (29) describes a Gaussian distribution whose centre of mass convects at speed U, whose peak concentration decays as $(Et)^{-1/2}$ and whose half width increases as $(Et)^{1/2}$.

For the numerical experiments the initial conditions cannot be set at time zero as an instantaneous point source cannot be resolved by a computational grid. The initial conditions have been defined at time t_0 when the half width of the distribution has grown to $B\,\Delta x$, where B is a dimensionless constant and a measure of the steepness of the initial profile. The peak concentration at this time has been set at 1·0. The half width of the distribution is the distance b such that

$$C(\bar{x} \pm b, t) = \tfrac{1}{2}C(\bar{x}, t) \tag{31}$$

i.e. the distance from the peak concentration to the points where the concentration has fallen to half the peak value. From equation (29)

$$b^2 = \frac{4Et}{\ln 2} \tag{32}$$

The half width is a more identifiable dispersion length scale than the standard deviation $(4Et)^{1/2}$, which appears naturally in equation (29).

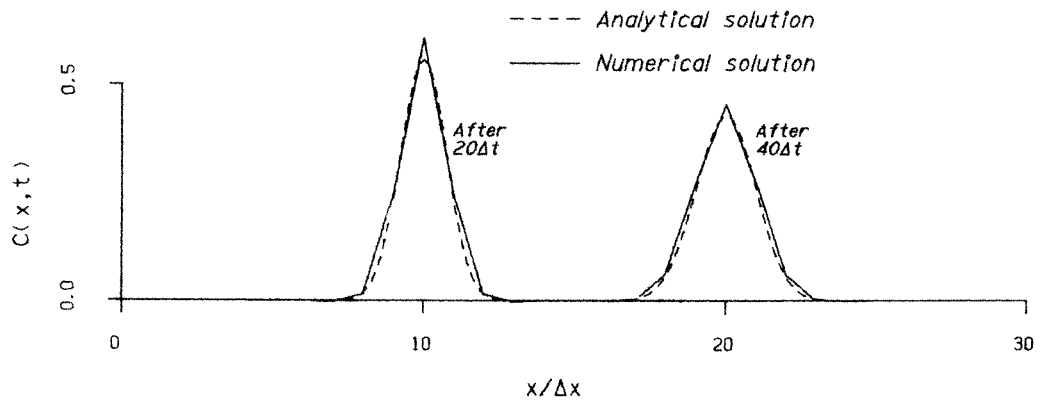

Figure 6. Steady flow numerical experiment for fractional step algorithm

For the numerical experiments included as Figures 6 to 8, the dimensionless initial half width is 0·5, which is quite extreme and almost beyond the resolution capabilities of the grid. Any numerical problems at short wavelengths will certainly be exposed by these initial conditions. The dispersion parameter for these experiments is 0·01, a typical value and sufficiently small that convection remains the dominant physical transport process. Figure 6 is a result for steady flow on a uniform grid ($A = 0{\cdot}0$). The flow parameter is 0·5 and the analytical and numerical solutions are compared after twenty and forty time steps. The peak concentration is slightly overpredicted at both times but the overall agreement is excellent. Figure 7 is the equivalent result at the same flow parameter for the Eulerian grid algorithm introduced above for comparative purposes. This result illustrates the classic problems of numerical dispersion and solution oscillations for Eulerian schemes, that were related above to the poor phase response of the algorithm. A comparison of Figures 6 and 7 readily confirms the excellent performance of the fractional step algorithm.

The final result, Figure 8, simulates an unsteady estuarine flow with

$$U(x, t) = U_F + U_T \sin(\omega t - kx) \tag{33}$$

U_F is a constant fresh-water component, U_T is the amplitude of the periodic tidal component, k is the wave number and ω the angular frequency of the tidal wave. The parameters

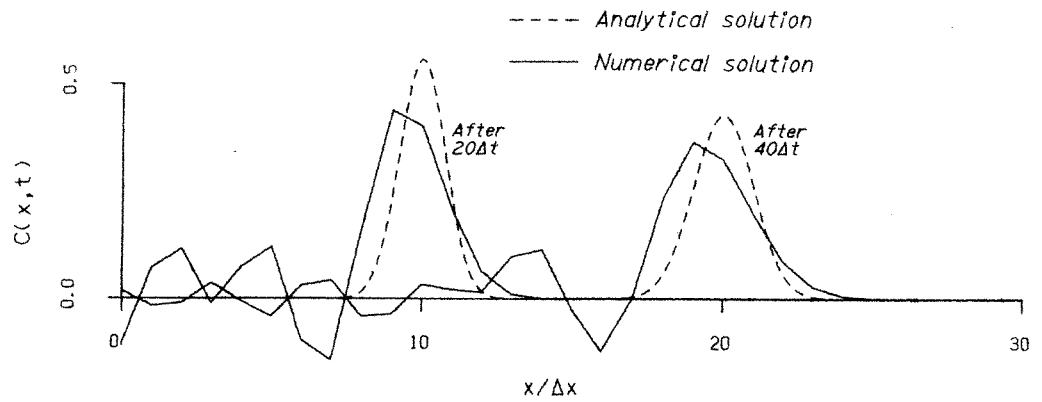

Figure 7. Steady flow numerical experiment for Eulerian grid

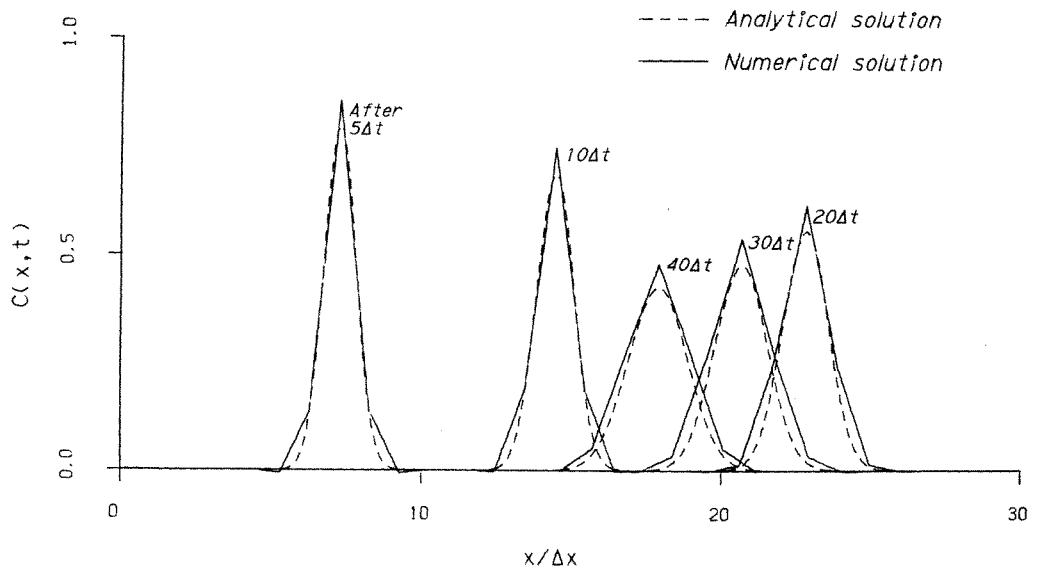

Figure 8. Unsteady flow numerical experiment for fractional step algorithm

were chosen as representative of estuarine conditions; the fresh-water flow parameter $U_F \Delta t/\Delta x$ was set at 0·5, the tidal flow parameter $U_T \Delta t/\Delta x$ at 1·0, the wave number at $2\pi/(750\,\Delta x)$ and the angular wave frequency at $2\pi/(50\,\Delta t)$. The initial conditions and dispersion parameter are as before. Under these conditions the flow changes direction periodically and varies with both position and time throughout the flow field. Under such conditions the grid asymmetry also varies with both position and time, providing a quite demanding test of the performance of the fractional step algorithm. The Figure 8 result is very good. There remains, as in Figure 6, some overprediction at the peaks which is a direct consequence of the predominance of short wave lengths in the quite extreme initial conditions. Less extreme initial conditions, a larger half width and/or a smaller space step, lead to an even better result.

DISCUSSION

There is an extensive literature on the numerical solution of equation (6), especially the primitive form that drops the reaction terms. It is a central problem in heat transfer (forced convection), mass transfer (pollutant transport in estuaries and rivers) and momentum transfer (Navier–Stokes equations) but the source of the numerical difficulties remains unchanged, being the convective term where the flow parameter is large (of order 1) and the dispersion parameter is small ($\ll 1$). The potential consequences are numerical dispersion and solution oscillations.

A number of recent reviews[10,11] have attempted to bring some perspective to the literature. In particular, Gresho and Lee [10] concentrate on Eulerian, finite element algorithms but their comments are generally relevant to all Eulerian representations (finite element, finite difference and method of characteristics). Their conclusions are clear, timely and compelling. They argue that solution oscillations ('wiggles') are symptomatic of a deeper numerical and/or physical problem in the solution formulation. Algorithms specifically designed to smooth the oscillations on coarse grids are rejected as the smoothed numerical

solutions do not necessarily represent solutions of the original partial differential equation. In this context, considerable attention was given to 'smart' upwinding techniques[12,13] which yield exact solutions at the nodes for steady-state convection– dispersion through knowledge of an exact local solution to the partial differential equation. Sobey and Vidler[14] have shown that a similarly exact approach is not possible for the transient convection–dispersion equation; Gresho and Lee reach the same conclusion from a more qualitative viewpoint. They argue that the solution oscillations are suppressed by numerical dispersion, so that upwinding is a reasonable approach only where both the flow parameter and the grid size are small, which is not a common situation. Despite the extensive literature, Gresho and Lee recommend the exclusive use of the conventional Galerkin finite element method (rather than inconsistent weighted residuals formulations) coupled with judicious mesh selection and refinement, taking maximum advantage of the flexibility (and high overheads) of common finite element software and living with solution oscillations.

It is clear that lowest order Eulerian algorithms (finite difference, finite element, method of characteristics) are unsatisfactory unless the grid is particularly fine, especially where concentration gradients are sharp. Higher order algorithms will improve the precision but there is a computational cost and (smaller) solution oscillations will persist. The numerical difficulties originate from discrete approximations to the convective term in an Eulerian framework. These difficulties are specifically avoided in the present fractional step algorithm by the adoption of the moving co-ordinate system for the convection step leading, through the method of characteristics, to an exact solution. This convection step introduces no numerical dispersion and no solution oscillations. The only potential error source is the prediction of the characteristic paths, but this is not a new problem as an equivalent computation is implicit in any Eulerian algorithm. The present formulation is in fact potentially superior as it is decoupled from equation (6). In the numerical integration of equation (16), Q and A are interpolated from the results of a preceding (fixed grid) hydrodynamic stage which may use a finer grid than the mass transport stage, although this will rarely be necessary for estuarine flows where Q and A are slowly varying functions of position and time for typical space steps (5000 m) and time steps (15 min). This aspect of the fractional step algorithm could be used to advantage in potential applications to rapidly reversing flows and to recirculating flows in two spatial dimensions.

In addition the fractional step algorithm is computationally efficient. Although there are three steps, none are numerically complicated. The reaction step, equation (12), is an explicit analytical result. The convection step has three stages, the first being the numerical integration of equation (16) to predict the characteristic paths using a Runge–Kutta algorithm of order consistent with the available predictions of Q and A; a first order algorithm was used in the successful predictions presented as Figures 6 and 8. The second stage, equation (17), is quite trivial and the third stage is the addition and removal of nodes. The dispersion step uses a lowest order algorithm whose accuracy (measured by the integrated square error) has been optimized for the asymmetric grid. The multi-step approach to each time step potentially increases the computational time with respect to a single step, lowest order Eulerian algorithm but this must be balanced against the significantly superior accuracy of the fractional step algorithm and its potential to maintain this precision on a coarse grid. Some relative measure of the computational efficiency of the fractional step algorithm is available from a direct comparison with two finite element algorithms from Reference 8. The test problem is the steady flow situation in Figures 6 and 7, the solution field comprising forty-five space steps and forty time steps. Both finite element algorithms are rectangular space-time elements; the first is the lowest order algorithm with $C^{0,0}$ nodal continuity and

linear shape functions (on which Figures 3 and 7 are based) and the second is a higher order algorithm with $C^{1,1}$ nodal continuity and first-order Hermitian shape functions. C.P.U. times on a DEC 1091 mainframe computer were 13·3, 30·4 and 237 s, respectively for the fractional step algorithm and the two finite element algorithms. The computational efficiency of the present fractional step algorithm is clear. Even allowing for the considerable software overhead in common finite element software, the fractional step algorithm is at least as efficient as the lowest order finite element algorithm which is significantly less acurate, and an order of magnitude more efficient than the higher order finite element algorithm which approaches comparable accuracy.

CONCLUSIONS

A successful and economical numerical solution algorithm has been developed for estuarine mass transport without recourse to higher order approximations. The algorithm uses the fractional step method, separating the convection–dispersion–reaction equation into consecutive fractional steps, reaction, convection and then dispersion. Essentially exact solutions are used for the reaction and convection steps, namely a local analytical solution for the reaction step and the method of characteristics along a moving co-ordinate system for the convection step. The dispersion step is accommodated by a lowest order but error optimized finite difference algorithm on the non-uniform grid that is a consequence of the moving co-ordinate system introduced in the convection step.

The convection step of the algorithm effectively eliminates numerical dispersion and solution oscillation difficulties that afflict many published algorithms, especially those that maintain an Eulerian grid. The Fourier response and integrated square error characteristics, together with numerical experiments, all confirm the excellent performance of the complete fractional step algorithm.

REFERENCES

1. N. N. Yanenko, *The Method of Fractional Steps*, English translation edited by M. Holt, Springer-Verlag, Berlin, 1971.
2. R. D. Richtmyer and K. W. Morton, *Difference Methods for Initial Value Problems*, 2nd edn., Wiley, New York, 1967.
3. I. R. Young and R. J. Sobey, 'The numerical prediction of tropical cyclone wind-waves', *Res. Bull. CS*20, *Dept. Civil & Systems Eng., James Cook Univ.*, 1981.
4. J. E. Fromm, 'A method for reducing dispersion in convective difference schemes', *J. Comput. Phys.* **3,** 176–189 (1968).
5. F. M. Holly and A. Preissman, 'Accurate calculation of transport in two dimensions', *J. Hydraul. Div. Am. Soc. Civ. Engrs.* **103,** 1259–1278 (1977).
6. R. J. Sobey, 'An optimised solution for the diffusion equation of a non-uniform grid', submitted for publication.
7. J. J. Leendertse, 'Aspects of a computational model for long-period water-wave propagation', *RM*-5294-*PR*, *Rand Corp., Santa Monica*, May, 1967.
8. R. J. Sobey, 'Hermitian space-time finite elements for estuarine mass transport', *Int. J. num. Meth, Fluids*, **2,** 277–297 (1982).
9. H. L. Stone and P. L. T. Brian, 'Numerical solution of convective transport problems', *A. I. Ch. E. Jl.* **9,** 681–688 (1963).
10. P. M. Gresho and R. L. Lee, 'Don't suppress the wriggles—they're telling you something'. *ASME AMD* **34,** 37–61 (1979).
11. R. J. Sobey, 'Numerical alternatives in transient stream response', submitted for publication.
12. I. Christie, D. F. Griffiths, A. R. Mitchell and O. C. Zienkiewicz, 'Finite element methods for second order differential equations with significant first derivatives', *Int. J. num. Meth. Engng.* **10,** 1389–1396 (1976).
13. T. J. R. Hughes, 'A simple scheme for developing "upwind" finite elements', *Int. J. num. Meth. Engng.* **12,** 1359–1365 (1978).
14. R. J. Sobey and P. F. Vidler, 'Numerical modelling of mass transport in well-mixed estuaries', *Res. Bull. CS*19, *Dept. Civil & Systems Eng., James Cook Univ.* (1980).